POF misalignment model based on the calculation of the radiation pattern using the Hankel transform

J. Mateo,[*] M. A. Losada, and A. López

GTF, Aragón Institute of Engineering Research (i3A), Department of Electronic Engineering, University of Zaragoza, María de Luna 1, E-50018 Zaragoza, Spain
[*]jmateo@unizar.es

Abstract: Here, we propose a method to estimate misalignment losses that is based on the calculation of the radiated angular power distribution as light propagates through space using the fiber far field pattern (FFP) and simplifying and speeding calculations with the Hankel transform. This method gives good estimates for combined transversal and longitudinal losses at short, intermediate and long offset distances. In addition, the same methodology can be adapted to describe not only scalar loss but also its angular dependence caused by misalignments. We show that this approach can be applied to upgrade a connector matrix included in a propagation model that is integrated into simulation software. This way, we assess the effects of misalignments at different points in the link and are able to predict the performance of different layouts at system level.

References and links

1. N. Antoniades, M. A. Losada, J. Mateo, D. Richards, T. K. Truong, X. Jiang, and N. Madamopoulos, "Modeling and characterization of SI-POF and connectors for use in an avionics system," in *Proceedings of 20th Intl. Conf. on Plastic Optical Fibres and Applications*, pp. 105–110 (2011).
2. A. Esteban, M. A. Losada, J. Mateo, N. Antoniades, and A. López, "Effects of connectors in SI-POFs transmission properties studied in a matrix propagation framework," in *Proceedings of 20th Intl. Conf. on Plastic Optical Fibres and Applications*, pp. 341–346 (2011).
3. M. A. Losada, F. A. Domínguez-Chapman, J. Mateo, A. López, and J. Zubia, "Influence of termination on connector loss for plastic optical fibres," in *Proceedings of 16th Intl. Conf. on Transparent Optical Networks*, paper Mo.C7.4 (2014).
4. D. Marcuse, "Loss analysis of single-mode fiber splices," Bell Syst. Tech. J. **56**(5), 703–718 (1977).
5. S. Nemoto and T. Makimoto, "Analysis of splice loss in single-mode fibres using a Gaussian field approximation," Opt. Quantum Electron. **11**(5), 447–457 (1979).
6. D. Gloge, "Offset and tilt loss in optical fiber splices," Opt. Quantum Electron. **55**(7), 905–916 (1976).
7. W. van Etten, W. Lambo, and P. Simons, "Loss in multimode fiber connections with a gap," Appl. Opt. **24**(7), 970–976 (1985).
8. C. Gao and G. Farrell, "Power coupling between two step-index multimode fibers of different numerical apertures with an angular misalignment," Microw. Opt. Technol. Lett. **43**(3), 231–234 (2004).
9. J. Mateo, M. A. Losada, N. Antoniades, D. Richards, A. López, and J. Zubia, "Connector misalignment matrix model," in *Proceedings of 21st Intl. Conf. on Plastic Optical Fibres and Applications*, pp. 90–95 (2012).
10. S. Werzinger, C. A. Bunge, S. Loquai, and O. Ziemann, "An analytic connector loss model for step-index polymer optical fiber links," J. Lightwave Technol. **31**(16), 2769–2776 (2013).
11. J. Mateo, M. A. Losada, I. Garcés, and J. Zubia, "Global characterization of optical power propagation in step-index plastic optical fibers," Opt. Express **14**(20), 9028–9035 (2006).
12. D. Richards, M. A. Losada, N. Antoniades, A. López, J. Mateo, X. Jiang, and N. Madamopoulos, "Modeling methodology for engineering SI-POF and connectors in an avionics system," J. Lightwave Technol. **31**(3), 468–475 (2013).
13. E. Grivas, D. Syvridis, and G. Friedrich, "Influence of connectors on the performance of a VCSEL-based standard step-index POF link," IEEE Photon. Technol. Lett. **21**(24), 1888–1890 (2009).

14. J. Mateo, M. A. Losada, and J. Zubia, "Frequency response in step index plastic optical fibers obtained from the generalized power flow equation," Opt. Express **17**(4), 2850–2860 (2009).
15. J. Xu, M. Bloos, and H. Poisel, "Improved modelling of connector losses for SI-POF based on exact values for the radiance at fiber end faces," in *Proceedings of 16th Intl. Conf. on Transparent Optical Networks*, paper Mo.C7.4 (2014).
16. N. Baddour, "Operational and convolution properties of two-dimensional Fourier transforms in polar coordinates," J. Opt. Soc. Am. A **26**(8), 1767–1777 (2009).
17. O. Ziemann, J. Krauser, P. E. Zamzow, and W. Daum, *POF handbook*, 2nd ed. (Springer, 2008).
18. M. A. Losada, J. Mateo, and A. López, "Matrix model of optical power propagation in plastic optical fibres," in *Proceedings of 12th Intl. Conf. on Transparent Optical Networks*, paper We.C3.3 (2010).

1. Introduction

Fiber misalignments are not unusual in splices and connectors where they constitute one of the main causes for power loss. These effects are particularly accentuated for plastic optical fibers (POFs) where the lower demands imposed to connectors imply larger error margins. Moreover, the deployment of POF requires a large number of connectors which is particularly critical in avionics systems [1]. In these networks, the presence of several connectors, whose insertion loss is usually higher than 1 dB [2,3], reduces significantly the power budget. Some misalignments are difficult to avoid when inserting the connectors as a tight control over the fibers can be expensive and troublesome. In addition, large fiber separation can be intentionally introduced as that in air-gap connectors. Vibrations, frequent in transportation network environments, are also the source of statistically variable positional mismatches. All these effects can add together introducing severe global limitations limiting further the already compromised power budget.

Most of the models for misalignment loss [4–8] assess each individual misalignment individually which prevents an accurate description of their combination as there is a strong non-linear dependence between them. Also, most models assume that the power radiated by the fiber takes a uniform distribution at any distance that renders them simple at the cost of poor accuracy, particularly for shorter (less than 100 microns) longitudinal separations that are the more likely to happen between connectors. In fact, the fiber radiated power distribution is a key point to predict misalignment losses. Thus, a more realistic approach is to estimate the radiated pattern from the far field pattern (FFP) emitted by the fiber as proposed in [9, 10]. In this later work, the calculation of misalignment loss requires an analytical FFP which was assumed to be the equilibrium mode distribution (EMD). However, for most POF systems the EMD can only be reached after more than a hundred meters [11], which is a distance well over the usual link length and, moreover, fiber union by connectors or splices can be needed at any position in the link [12,13].

In this paper, we formalize and optimize the method we proposed in [9] where the radiated angular power distribution is calculated as the convolution of the fiber aperture and its far field pattern (FFP), applying the Hankel transform to simplify and speed calculations. Thus, our approach is capable to handle several combined misalignments while having the flexibility to accommodate different analytical functions or even measured FFPs which will permit to obtain misalignment loss for any input conditions and at any point at the link. However, misalignments cause not only overall loss, but also introduce changes in the shape of the angular power distribution. Therefore, we also present a similar methodology applied to obtain the effect of the misalignments as a function of the propagation angle. These calculations are independent of the shape of the FFP and provide a qualitative assessment of the angular-dependent power loss caused by different misalignments that can be used to predict its impact on transmission properties. Moreover, the functions obtained are used to upgrade a basic connector model in the context of the propagation matrix framework that describes the power loss and the diffusion introduced by a double-connector including misalignments [12].

The paper is organized as follows: first, the model is described stating the initial assumptions and simplifying the calculations using the Hankel transform to obtain power loss.

Second, following this approach, we obtain an analytical description of the relative change in power as a function of the angle for different misalignments. Then, we present the model results for combined longitudinal and transversal misalignments and show how the angular-dependent power loss caused by misalignments can be very useful to evaluate their impact over transmission properties in the context of the matrix propagation model [14]. Finally, we summarize our proposal focusing on its flexibility to accommodate other fibers, effects and conditions.

2. Theoretical development

2.1 Calculation of misalignment power loss

In this subsection, we propose a method to obtain the power loss incurred when there are combined transversal and longitudinal offsets between two plastic optical fibers by calculating the fraction of the power distribution radiated from the radiating fiber that is caught by the receiving fiber. We assume some previously admitted hypotheses [9,10,15]:

    i) Each point in the first fiber end surface acts as an independent uncorrelated source. All these sources are identical which is equivalent to model the fiber end surface as a circular aperture with a real uniform transmission function.

    ii) The radiation of each source point is described by the fiber far field pattern (FFP) which is constrained to have circular symmetry.

    iii) The total power at a given point in the space is obtained by adding the scalar contributions (optical powers) from all radiating sources that reach that point.

    iv) The power captured by the receiving fiber is obtained as the fraction of power radiated from the first fiber that overlaps with the core surface of second fiber.

    v) Another function has to be introduced to account for the difference in the power captured by the receiving fiber, depending on its angle of incidence. We call it differential efficiency function and model it using the FFP of the receiving fiber.

Notice that hypotheses i) to iii) relate to the radiating fiber and to how power distribution spreads as it propagates in free space while iv) and v) relate to the receiving fiber geometry and its physical capability to capture light.

Next, we show how the power distribution radiated from the fiber at any point in the space can be obtained as the 2D convolution of the fiber aperture function and its far field pattern whose calculation can be simplified using the Hankel transform providing both functions are circularly symmetric. Then, the power transferred to the receiving fiber is obtained by integrating the power distribution radiated from one fiber over the other fiber surface.

The first step is to obtain the radiated optical power distribution R at different distances z of the emitting fiber. Taking into account the fiber symmetry, we choose to work in cylindrical coordinates (r, φ, z) centered on the axis of the emitting fiber (OO' in Fig. 1), where r is the axial distance, φ is the angle relative to the fiber axis, and z is the distance to the fiber end face along its axis. Thus, the power distribution can be represented as $R(r, \varphi, z)$. One of our assumptions, fundamental to apply a fast method to ease the calculations, is that the fiber has circular symmetry and consequently, the emitted power distribution R is independent on φ. Therefore, from now on we will refer to it as $R(r, z)$.

For the calculation of the optical power distribution we have assumed that the points on the core surface of the emitting fiber are individual sources and that all have the same radiation pattern. Thus, we represent the emitting surface at $z = 0$ as a circle of radius a, and unit amplitude, given by:

$$C(r_1, \varphi_1) \equiv C(r_1) = \begin{cases} 1, r_1 \leq a \\ 0, r_1 > a \end{cases} \qquad (1)$$

Therefore, any point at the end face of the fiber, $A \in C(r_1, \varphi_1)$ radiates light with a power density given by the fiber FFP, $g(\theta)$, whose only dependence is on θ, that is the propagation angle relative to the fiber axis. The power distribution over a plane at a distance z from the fiber end is given by the projection of the FFP onto this plane. Thus, the amount of radiation from each point source A that reaches B is determined by the angle θ between A, B and A', that is the projection of A on the plane perpendicular to the fiber axis that contains B. These assumptions are illustrated in Fig. 1.
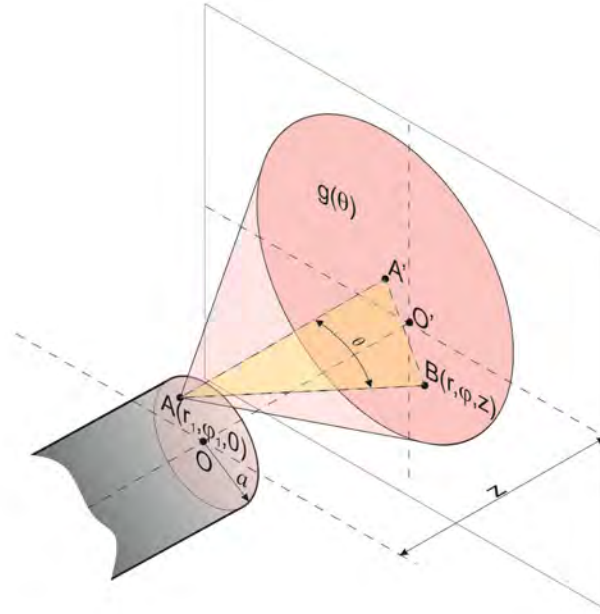

Fig. 1. Schematic of the geometry of power radiation from the fiber end surface. The power radiated from A that reaches B is given by g (θ), where θ is the angle defined by A, A' and B.

Then, the optical power over a point B in the space with coordinates (r, φ, z) is obtained by adding the uncorrelated contributions from all the source points on the circular surface of the radiating fiber which is calculated as the integral over the emitting circle $C(r_1, \varphi_1)$ of the projection of the FFP onto the plane containing B. This integral is given by:

$$R(r, z) = \int_0^{2\pi} \int_0^{\infty} C(r_1, \varphi_1) g\left(\theta(r_1, \varphi_1, r, \varphi, z)\right) r_1 dr_1 d\varphi_1. \qquad (2)$$

Using basic trigonometric relationships, angle θ can be expressed in terms of the cylindrical coordinates of any point $A(r_1, \varphi_1)$, on the fiber core surface and $B(r, \varphi, z)$, on the perpendicular plane at distance z from the fiber:

$$\theta = \tan^{-1}\left(\frac{\sqrt{r_1^2 + r^2 - 2r_1 r \cos(\varphi_1 - \varphi)}}{z}\right). \qquad (3)$$

Introducing this relationship in Eq. (2), the power distribution $R(r, z)$ is given by the following expression:

$$R(r,z) = \int_0^{2\pi} \int_0^a g\left(\tan^{-1}\left(\frac{\sqrt{r_1^2 + r^2 - 2r_1 r \cos(\varphi_1 - \varphi)}}{z} \right) \right) r_1 \, dr_1 \, d\varphi_1. \tag{4}$$

Notice that even though all functions have rotational symmetry, there is a dependence on the angles φ and φ_1 that makes this integral tedious to calculate. However, Eq. (4) is exactly the two-dimensional convolution of the circle and the FFP expressed in cylindrical coordinates. The former result is quite intuitive as it is reasonable to expect that to obtain the power at a given point we have to add the shifted contributions from all points at the radiating fiber surface, as is illustrated in Fig. 2.
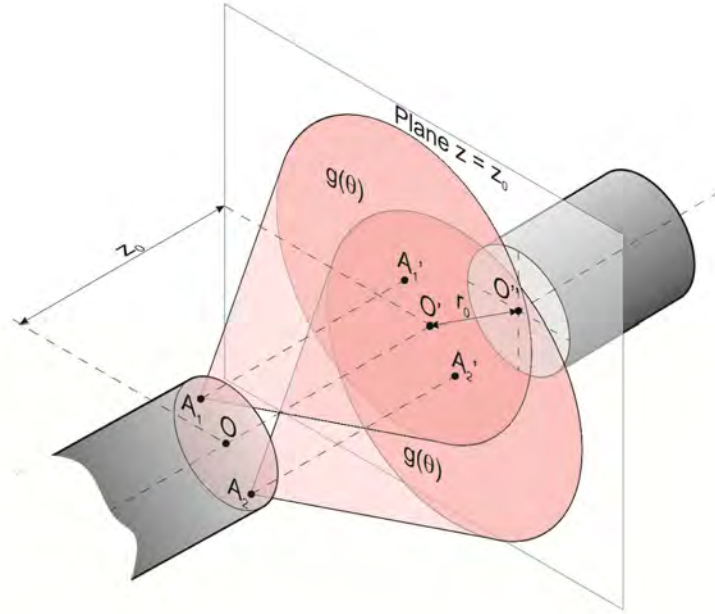

Fig. 2. The radiated power from all points at the radiating fiber end surface is superposed to obtain the total power at plane z = z_0, where the receiving fiber is placed.

The key point is that the 2D convolution of two circular symmetric functions can be simplified using the Hankel transform of order 0 [16]. In the transformed domain, the convolution is computed as the product of the transforms of $C(r)$ and the scaled FFP that are both functions of ρ. Then, we can obtain the power distribution $R(r, z)$ as the inverse Hankel transform of the product given by:

$$R(r,z) = C(\vec{r}) ** g(\vec{r}) = C(r) ** g\left(\frac{r}{z}\right) = z^2 \cdot \mathrm{H}^{-1}\left\{ \frac{a\, J_1(2\pi a\rho) \cdot G(z\rho)}{\rho} \right\}, \tag{5}$$

where H^{-1} is the inverse zero-order Hankel transform, $G(\rho)$ is the transform of $g(r)$, and $a \cdot J_1(2\pi a\rho)/\rho$ is the Airy pattern that is the transform of a circular aperture with radius a. We have applied the similarity property of the Hankel transform: $h(sr) \leftrightarrow s^{-2} \mathrm{H}(\rho/s)$ to obtain $\mathrm{H}\{g(r/z)\}$.

Once the radiated power distribution $R(r, z)$ given in Eq. (5) has been obtained, it can be used to calculate the fraction of the power radiated from the first fiber that is coupled into the second fiber when the two fibers have both longitudinal (z_0) and transversal (r_0) offsets as shown in Fig. 2, applying hypotheses iv) and v). The first hypothesis implies that the fraction of the power emitted from the emitting fiber that falls on the core surface of the other fiber is

captured while the rest is lost. Thus, the relative power coupled to a fiber of radius a centered at coordinates (r_0 , z_0) is given by the integral of the radiated power distribution projected on the plane: $z = z_0$: $R(r_0 , z_0)$, over the circular surface, C', of the receiving r_0-shifted fiber:

$$P(r_0, z_0) = \iint_{C'} R(r, z_0) r \, dr \, d\varphi, \tag{6}$$

where C' is defined by: $C'(r) = \begin{cases} 1, r - r_0 \leq a \\ 0, r - r_0 > a \end{cases}$.

The cylindrical coordinates of the integral are again relative to the emitting fiber axis. Thus, the limits in r for this integral are different depending on the relative valued of the shift r_0 and the receiving fiber radius a which makes necessary to consider the cases: $r_0 < a$ and $r_0 > a$ separately. The integration in φ can be performed in both cases obtaining its limits as a function of r, r_0 and a using the cosine rule.

$$P(r_0, z_0) = \begin{cases} \dfrac{2\int_{r_0-a}^{r_0+a} \cos^{-1}\left(\dfrac{r_0^2 + r^2 - a^2}{2rr_0}\right) R(r, z_0) r \, dr}{2\pi \int_0^\infty R(r, z_0) r \, dr}, \text{ if } r_0 \geq a \\[3em] \dfrac{2\pi \int_0^{a-r_0} R(r, z_0) r \, dr + 2\int_{a-r_0}^{a+r_0} \cos^{-1}\left(\dfrac{r_0^2 + r^2 - a^2}{2rr_0}\right) R(r, z_0) r \, dr}{2\pi \int_0^\infty R(r, z_0) r \, dr}, \text{ if } r_0 < a \end{cases} \tag{7}$$

It remains to introduce the differential efficiency of the receiving fiber to capture light depending on the input angle (hypothesis v) in Eq. (4). In that equation, $g(\theta)$ was used to represent the FFP of the emitting fiber that is the amount of power emitted at each angle. If the fiber axes are parallel, the power exiting the radiating fiber with a given angle, will reach the other fiber at this same angle. Thus, we model this efficiency as the FFP of the receiving fiber. Therefore, from now on, $g(\theta)$ will be the product of the FFPs of the emitting fiber, $g_1(\theta)$, and the FFP of the receiving fiber, $g_2(\theta)$: $g(\theta) = g_1(\theta) \cdot g_2(\theta)$. In this way, the loss of joining fibers with different apertures can be obtained in combination with misalignments. Otherwise, if both fibers are equal, $g(\theta)$ will be the squared fiber FFP. In any case, this enhancement does not introduce further calculations due to the use of the Hankel transform.

We want to stress that this method has ample flexibility as the Hankel transform of the far field pattern, $G(\rho)$ is tabulated for most functions proposed to model the FFP (uniform, Gaussian, etc.), but can also be obtained for experimental or non-analytical FFPs provided they have circular symmetry and can be described by their radial profiles. However, any change in the shape of the FFP will imply to re-calculate the radiation power distribution by Eq. (5) and then, applying Eq. (7) to obtain actual losses. Moreover, the method gives scalar power loss but its angular dependence is not retained. Thus, in the next subsection we describe a framework that gives, not only the absolute power loss produced by fiber misalignments, but also its angular variation while it does not require advanced knowledge of the shape of the FFP.

2.2 Calculation of angular-dependent power loss

In this subsection, our aim is to offer a new tool to describe the changes in power distribution that are caused by combined longitudinal and transversal shifts. Thus, we propose an approach similar to that described in Subsection 2.1, keeping assumptions i), ii) and iv) while it is not necessary to know either the emitting or the receiving fiber FFPs. In this case, we calculate the proportion of light that, exiting the radiating fiber *only* at a given angle θ_r, is able to reach the receiving fiber. This is equivalent to assume that each point of the fiber radiates light in a very narrow angular range $d\theta$ centered at θ_r that can be ideally represented with a

delta function as $\delta(\theta-\theta_r)$. Then, instead of a circular pattern, its projection onto a perpendicular plane will be a very narrow ring, as depicted in Fig. 3. Notice that any rotational symmetric pattern can be represented on the plane as a linear combination of these rings for different angles.
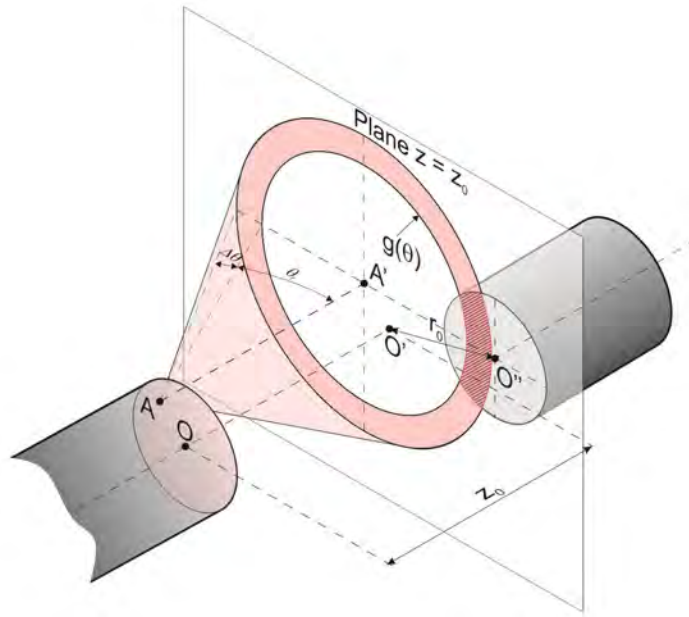

Fig. 3. Schematic that shows the fiber radiating light only at a specific direction given by angle θ_r and the projection of the radiation pattern onto the plane of the second fiber.

The radiated power distribution is then calculated by convolving the circular aperture of the emitting fiber with the narrow ring described by its radius: $z\tan(\theta_r)$. As circular symmetry is still maintained, the Hankel transform can be used to simplify these calculations. In fact, its use is paramount as otherwise a double integral will have to be calculated for each angle θ_r while we only have to obtain the product of two functions and its inverse transform.

Thus, following the same procedure as in Eqs. (2) to (5), the power distribution over a plane at a distance z of the power radiated at angle θ_r by the emitting fiber is given by the following equation:

$$R(\theta_r,r,z) = 2\pi z\tan(\theta_r)a^2 \cdot H^{-1}\left\{\frac{J_1(2\pi a\rho)}{a\rho} \cdot J_0(2\pi z\tan(\theta_r)\rho)\right\}, \qquad (8)$$

where $a\cdot J_1(2\pi a\rho)/\rho$ is again the Airy pattern and $2\pi z\tan(\theta_r) J_0(2\pi z\tan(\theta_r)\rho)$ is the Hankel transform of a delta function: $\delta(r-b) \leftrightarrow 2\pi b J_0(2\pi b\rho)$ with $b = z\tan(\theta_r)$.

Finally, the fraction of the power emitted at a given angle, θ_r, that falls on the core surface of the other fiber is obtained for each pair (r_0, z_0) applying the same procedure described in Subsection 2.1, but to $R(\theta_r, r, z)$ instead of to $R(r, z)$. It simply consists in substituting $R(r, z)$ by $R(\theta_r, r, z)$ in Eq. (7) and implies to calculate the integral for each θ_r. In this way, the function obtained does not only depend on the misalignments, but also on the propagation angle: $P(\theta_r, r_0, z_0)$. This function represents the proportion of power propagating at angle θ_r, that is transferred to the receiving fiber when it is shifted at (r_0, z_0). Therefore, it can be used to obtain the angular-dependent power loss imposed by any pair of misalignments. As in the case of POFs spatial changes are very much entangled to their temporal behavior, they can have important consequences on the fiber transmission as will be demonstrated in Subsections

3.3 and 3.4 with a specific application to incorporate the effects of misalignments into a connector matrix model and predict transmission parameters under different conditions.

In addition, the conclusions derived from this function are general in the sense that no assumptions have been made on the shape of the FFP of the fibers involved. In fact, $P(\theta_r, r_0, z_0)$ can be treated as a kernel to obtain the power transferred to the receiving fiber for a given misalignment pair (r_0, z_0): $P(r_0, z_0)$ that was obtained before using Eq. (7). Now, once the user knows how to implement $g(\theta)$, the only calculation required to obtain the power coupled into a fiber placed at (r_0, z_0) will be the following integral:

$$P(r_0, z_0) = \int_0^{\pi/2} g(\theta) P(\theta, r_0, z_0) \sin(\theta) d\theta. \tag{9}$$

3. Results

3.1 Combined misalignment power loss

To demonstrate how the proposed method is able to predict losses for combined misalignments, the surface plot in the upper graph of Fig. 4 shows the power transferred from one fiber to another as a function of combined longitudinal and transversal offsets calculated using our method with a Gaussian FFP. Experimental measurements obtained with a 1 mm SI-POF are superimposed to these predictions as black dots [9].
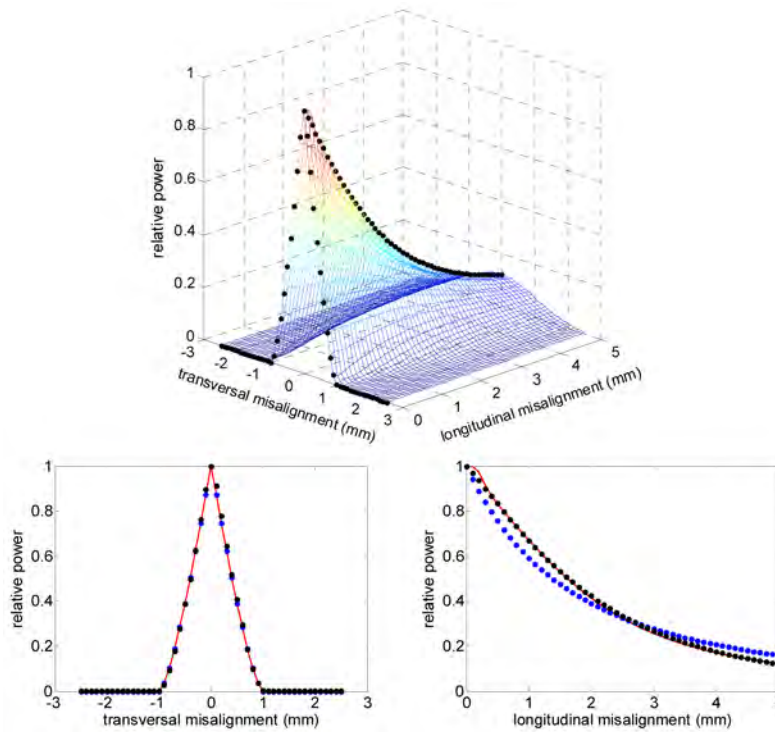

Fig. 4. The surface plot on the upper side represents the model prediction of the power transferred between two fibers with longitudinal and transversal offsets. Superimposed black dots are experimental measurements obtained shifting two fibers along the longitudinal and transversal axis. On the lower side, the predictions of our model (red lines) for transversal (left) and longitudinal (right) offsets are compared to predictions of the traditional model (blue circles) and experimental measurements (black circles).

The lower graphs show experimental measurements of the transmitted power separately for transversal (left) and longitudinal (right) offsets, respectively. They are compared to our predictions and to those obtained using the prevailing model described in [17] (pp. 261 and

266). While measurements for transversal offsets are well predicted by both models, our method provides a better representation of experimental data for longitudinal misalignments. The reason is that the initial decrease of transferred power with a longitudinal offset is not as steep as predicted by the traditional model. This model assumes that the radiated power has a uniform distribution that spreads with the numerical aperture (NA) of the fiber while our model predicts that power spreads at a lower rate with propagation, producing a better match. This demonstrates that the shape of the FFP used to calculate the radiation pattern determines not only its profile but also its dependence with length, both of which have an impact on the predicted misalignment losses. This is particularly important for POFs whose power distribution is strongly dependent on launching conditions and fiber type which added to their strong mode coupling and differential attenuation that produce rapid changes in power distribution with propagation distance [11]. In addition, it has been demonstrated that power distribution can be easily altered by curvatures and other localized disturbances. Therefore, the effects of misalignment for POFs can change drastically for different conditions and also depend on their position in the line as we will illustrate later in Subsection 3.3.

3.2 Angular-dependent power loss by combined misalignments

To generalize and make more flexible our proposal, we have obtained in Subsection 2.2 the power transferred between two shifted fibers for each propagation angle: $P(\theta_r, r_0, z_0)$, that can be calculated as shown in that subsection without making any assumptions on the shape of the FFP. Now, we will use this function to get further insight in the influence of the different misalignments on the power distribution. Figure 5 represents the angle-dependent transferred power $P(\theta_r, r_0, z_0)$ for three longitudinal misalignments: $z_0 = 0.1$ mm, 0.5 mm and 1 mm, alone and combined with four transversal misalignments, $r_0 = 0.25$ mm, 0.5 mm, 0.75 mm and 1 mm. These curves confirm that it is necessary to assess the combined effects of both misalignments as they are not independent. The graphs also show how, for increasing z-distances, power at higher angles is lost. This finding is consistent with previous reports that have indicated the effect of longitudinal shifts acting as a spatial filter that is able to increase bandwidth depending on its position in the link [12]. For r-shifts above 0.2 mm, losses are greater but relatively constant for small z distances. However, if the z-shift increases, the angular dependence is no longer constant and the relative power coupled from lower and higher angles changes depending on the transversal offset. In fact, for 1-mm shifts in both dimensions, power from higher angles is coupled to the other fiber while all power transmitted near the axis (0°) is practically lost. This is reasonable as, when the centers of the fibers are separated by large transversal shifts, only light radiated at the highest angles is able to reach the receiving fiber.

We want to stress that all the curves represented in Fig. 5 can be calculated without making initial assumptions, either on the shape for the fiber FFP or on its angular efficiency, and that the conclusions derived from them, are general and independent on other conditions.
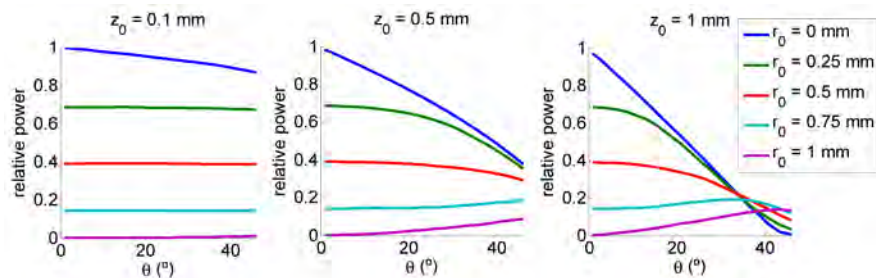

Fig. 5. Angle-dependent transferred power for three longitudinal z_0 and four transversal misalignments, r_0.

3.3 Generalized connector matrix

In recent works, we proposed a matrix framework to model light propagation in POFs where fiber attenuation and diffusion effects are described using the propagation matrix [14]. This matrix that is defined for each temporal frequency gives the amount of power in a given angle that is transferred to another angle. The optical power distribution transmitted through the fiber is described as a function of propagation angle and frequency. This approach was also extended to describe linear passive devices that produce power transfer among angles. In fact, we showed that connectors behave linearly and that a square matrix can describe not only their insertion loss, but also the changes over the angular power distribution [12]. In this way, a POF link can be simulated by the product of several matrices that model different fiber lengths and also the connectors that join them [18].

As misalignments and mismatches are frequent in the connected fibers, our aim here is to obtain an upgrade of the basic connector matrix $\mathbf{C}$, obtained for the best possible alignment [12], to incorporate also longitudinal and axial misalignments. In a previous work [9], our experimental results revealed that there is no increase in diffusion with misalignments, but only power loss that is angular dependent. Then, we incorporate the effects of two combined shifts (r_0, z_0) into the basic connector matrix for each particular angle by using function $P(\theta_r, r_0, z_0)$ conveniently sampled and put in vector form: $\mathbf{P}(r_0, z_0)$. Thus, the matrix $\mathbf{C}(r_0, z_0)$ for a misaligned connector can be obtained by the following product:

$$\mathbf{C}(r_0, z_0) = \mathbf{P}(r_0, z_0) \cdot \mathbf{C}, \qquad (10)$$

where the further angular-dependent loss produced by the misalignments is described by vector $\mathbf{P}(r_0, z_0)$, while the basic connector matrix $\mathbf{C}$ accounts for both attenuation and diffusion (mode mixing). Figure 6 shows the connector matrices for several misalignment pairs. Each matrix represents the amount of power that entering the connector with a given angle (x-axis) exits the connector spread over other angles (y-axis). Red indicates maximum power transfer while dark blue is none. All images are shown normalized to the maximum in the basic connector matrix, which is shown in the leftmost graph for a polished ST connector [12].

As expected, these images illustrate how these misalignments not only increase the overall connector insertion loss, but alter even further the angular power distribution. The right hand matrices reveal how larger shifts produce higher losses, and also that different misalignment combinations introduce angular-dependent losses, thus changing the transmitted optical power distribution. Particularly, in the case of longitudinal offsets, power loss is very angle-dependent with higher angles suffering more attenuation. Moreover, these matrices are independent of the exact location of the misaligned connector and its calculation does not require making assumptions over the FFP of the emitting fiber or the angular efficiency of the receiving one, which is essential to the application example shown in the next subsection.
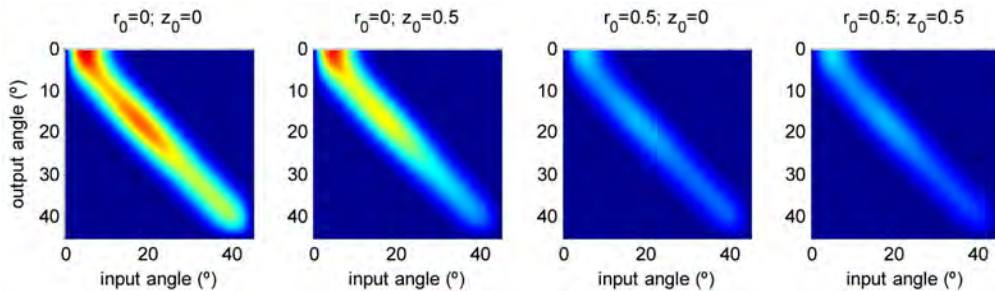

Fig. 6. Matrices for a polished ST connector. From left to right: basic matrix; 0.5 mm longitudinal offset; 0.5 mm axial offset and combined axial and longitudinal 0.5 mm offsets.

3.4 Integration into the matrix simulation environment

The generalized connector matrix can be integrated into the POF propagation matrix toolbox and used to incorporate the effects of connector misalignments. To illustrate the use of the connector matrix to evaluate the impact of misaligned connectors on a practical POF link, we analyze here a simple example of the use of all the previous theoretical developments. The schematic in Fig. 7 shows a 5-meter POF link that is implemented with or without a misaligned connector in two different possible positions. The results obtained with this example will also confirm the strong influence of input conditions over the consequences of misalignment.
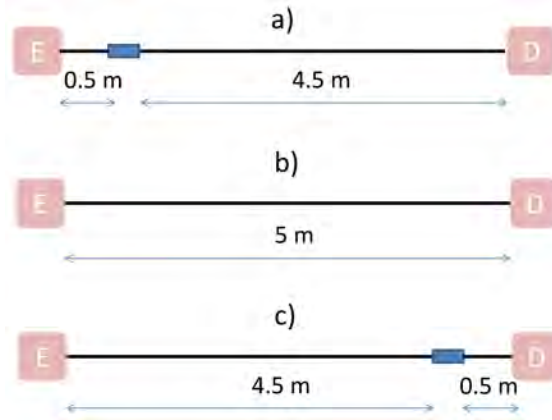

Fig. 7. Five-meter POF link with a) a connector at 0.5 m from the emitter; (b) without connectors and (c) with a connector at 4.5 m from the emitter. The connector is misaligned (r_0=0.5 mm, z_0=0.5 mm).

In our approach, vectors provide angular power distributions at different points in the link and matrices describe the diffusion and loss introduced by different fiber lengths or by misaligned connectors. The links shown in Fig. 7 are described by the following matrix products:

$$\text{a) } \mathbf{p}_D = \mathbf{M}_{0.5m} \cdot \mathbf{C}(0.5, 0.5) \cdot \mathbf{M}_{4.5m} \cdot \mathbf{p}_E$$
$$\text{b) } \mathbf{p}_D = \mathbf{M}_{0.5m} \cdot \mathbf{M}_{4.5m} \cdot \mathbf{p}_E \qquad , \qquad (11)$$
$$\text{c) } \mathbf{p}_D = \mathbf{M}_{4.5m} \cdot \mathbf{C}(0.5, 0.5) \cdot \mathbf{M}_{0.5m} \cdot \mathbf{p}_E$$

where $\mathbf{p}_E$ is the source angular distribution in vector form, and $\mathbf{p}_D$ the transmitted power distribution that reaches the detector. $\mathbf{M}_L$ is the propagation matrices that account for power loss and mode coupling caused by L fiber meters (in this case, L is 0.5 or 4.5 m). $\mathbf{C}(0.5, 0.5)$ is the upgraded connector matrix for longitudinal and transversal offsets of 0.5 mm. This matrix, shown in the rightmost graph of Fig. 6, describes not only the power loss and mode mixing introduced by a basic connector but also incorporates the angular-dependent power loss due to the combined misalignment. Both the fiber propagation matrix and the power distribution have dependences on the angle and the frequency, while the connector matrix only has angular dependence. As Eq. (11) shows, a change of the position of the connector in the link only affects the order of product operation but, as we soon will see, has a relevant impact on performance.

In Fig. 8, the amplitude transfer functions measured at the detector are compared for the three configurations. The left graph shows the simulation results when the source has a wide emission pattern such as a LED (with a FWHM of 30°) and the one on the right for a narrower source such as a VCSEL (10°). As all matrices are independent on the input

conditions, they do not have to be re-calculated to evaluate the link when the source is changed.
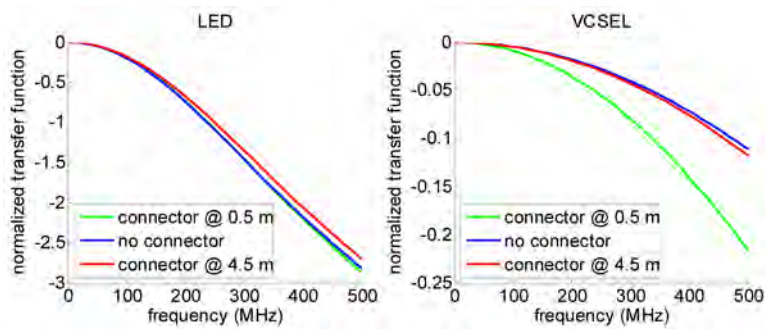

Fig. 8. Absolute value of the normalized transfer function measured at the detector for a LED (FWHM of 30°) on the left and a VCSEL (10°) on the right.

Although in this example overall connector loss is similar for both sources and positions (for the VCSEL: 5.53 dB and 5.40 dB for a) and c) respectively and 5.33 dB and 5.31 dB for the LED), their transfer functions are very different. A comparison of the right and left graphs shows how the presence of the connector degrades the performance in the case of a narrow source, particularly when the connector is near the source. For the LED, however, the presence of the connector near the detector actually improves the performance while the degradation introduced when it is near the source is very small. These effects are consequence of the changes in angular power distribution along the fiber that are intensified by the large misalignments in the connector. This example illustrates how connector misalignment can be critical in actual links and how it is difficult to use a general model based on fixed FFPs to predict their effects.

6. Conclusions

In this paper, we obtained the radiated power distribution as light propagates in free space from the end surface of a fiber in order to calculate the fraction of power that can be captured by another fiber depending on their relative positions. We showed that the radiated power distribution can be calculated as a 2D convolution simplified using the Hankel transform. Using this power distribution, we calculated misalignment power losses that gave good estimates for combined transversal and longitudinal offsets. We stress the simplicity of our approach and its adaptability that permits to incorporate fiber parameter mismatches (different radii or numerical aperture, lack of circularity, etc.) or misalignments along other axes (tilt, etc.). In addition, the approach has been used to upgrade a connector matrix in the context of the propagation matrix framework where fiber propagation and localized disturbances are described as matrices and, there is no need to make assumptions over the fiber FFP. While other models proposed so far are only able to predict global power loss the upgraded connector matrix also provides changes in angular power distribution. In addition, it can be easily introduced at any point of a POF link to provide an estimate of the performance for any initial conditions.

Acknowledgments